Supporting Information

Counter-ligand Control of the Electronic Structure in Copper-Tetrakisguanidine Complexes

A. Ziesak, T. Wesp, O. Hübner, E. Kaifer, H. Wadepohl, H.-J. Himmel*

Content

Figure S1. EPR spectrum of [**6**{Cu(OAc)$_2$}$_2$] in frozen CH_2Cl_2 at 35 K.

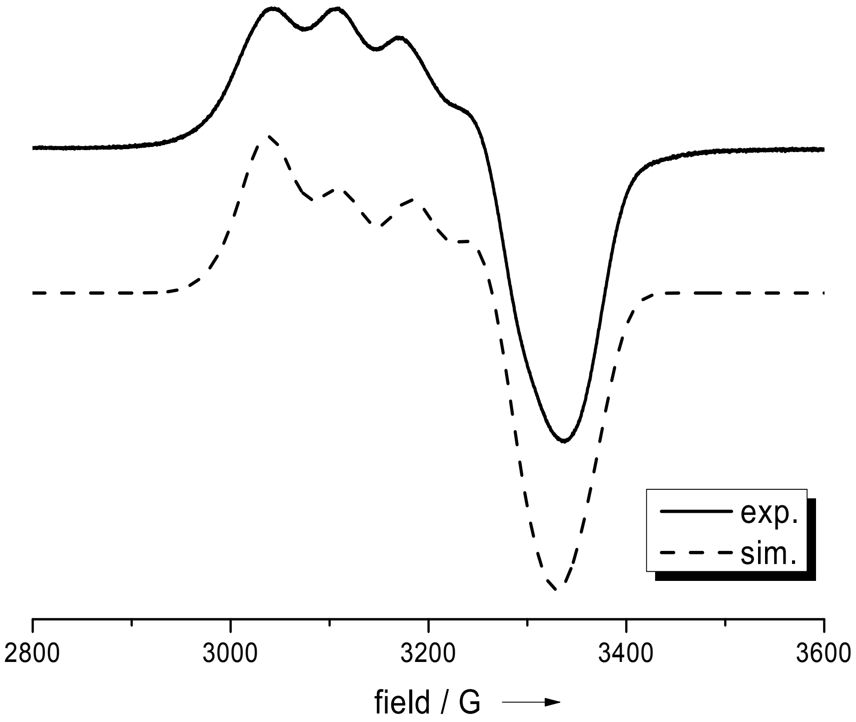

Figure S2. Magnetometric (SQUID) curve for [**6**($CuBr_2$)$_2$].

a) χ versus T curve at 500 and 1000 Oe.

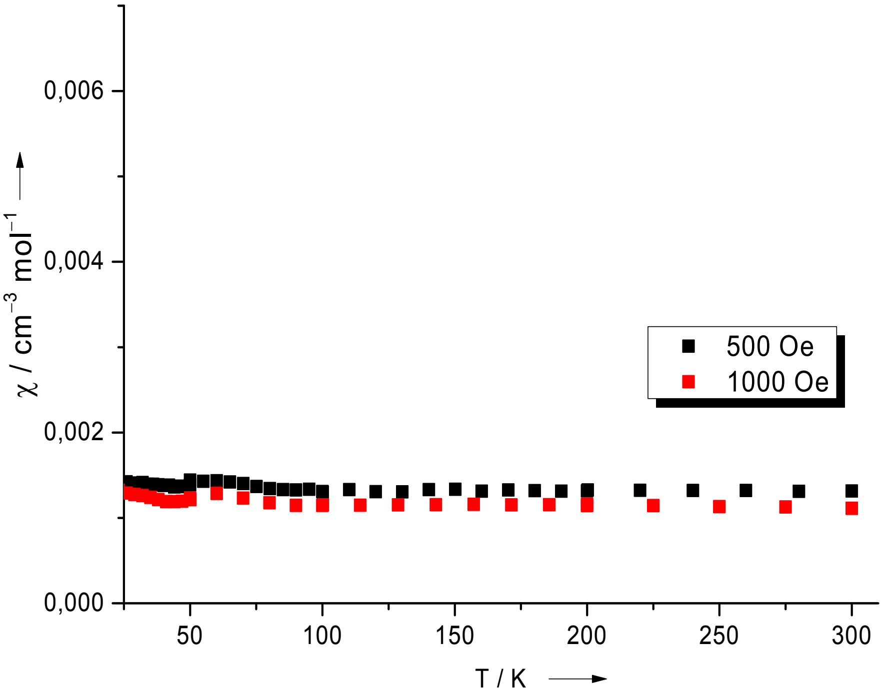

a) χ^{-1} versus T curve at 1000 Oe.

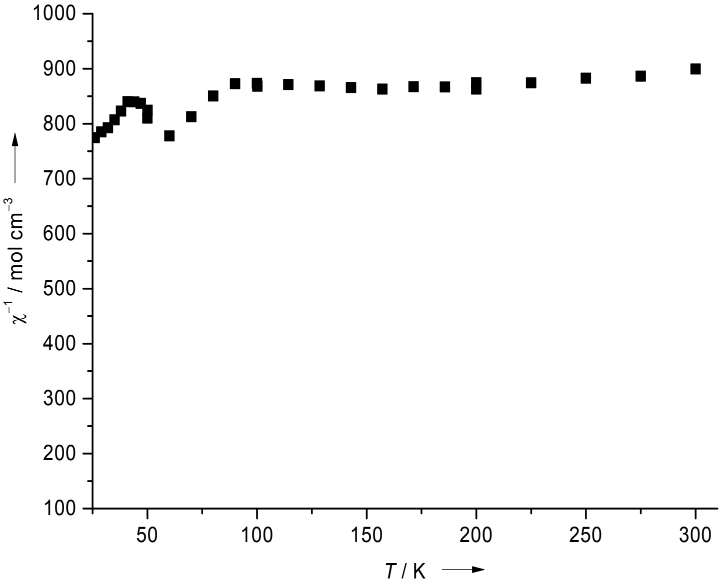

Figure S3. Cyclic voltammetry (CV) curves (scan rate 100 mV/s, supporting electrolyte [*n*Bu_4N](PF_6), Ag/AgCl, Fc/Fc^+) for a) [**6**{Cu(OAc)$_2$}$_2$] in CH_2Cl_2 and b) [**6**($CuBr_2$)$_2$] in CH_3CN.

a)

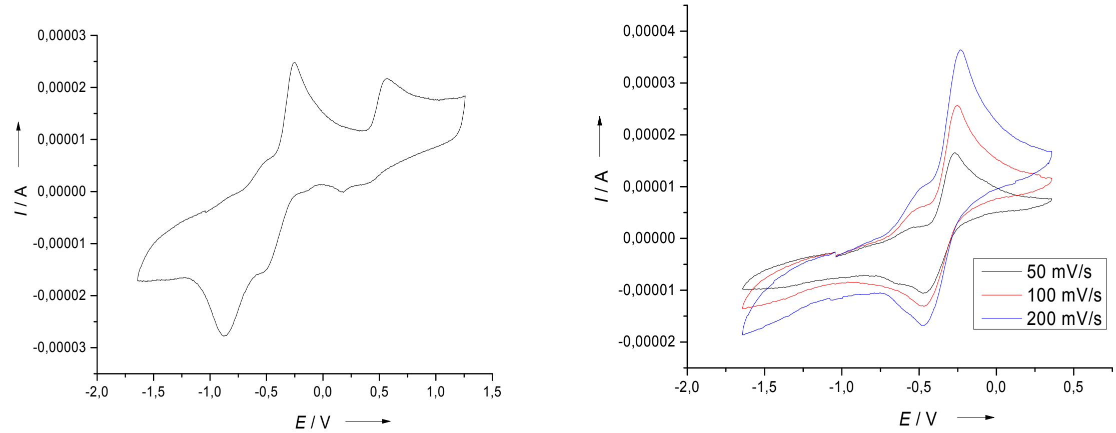

b)

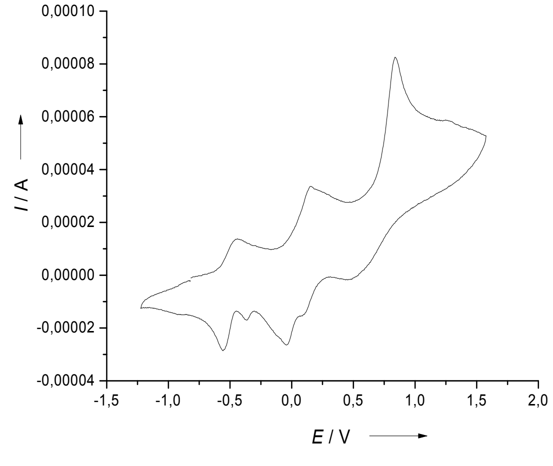

Figure S4. a) IR spectra of [**6**(CuBr$_2$)$_2$] and [**6**{Cu(OAc)$_2$}$_2$] (KBr disc). b) Comparison between the IR spectra of **6**, **6**$^{2+}$(I$_3^-$)$_2$ and [**6**(CuBr$_2$)$_2$].

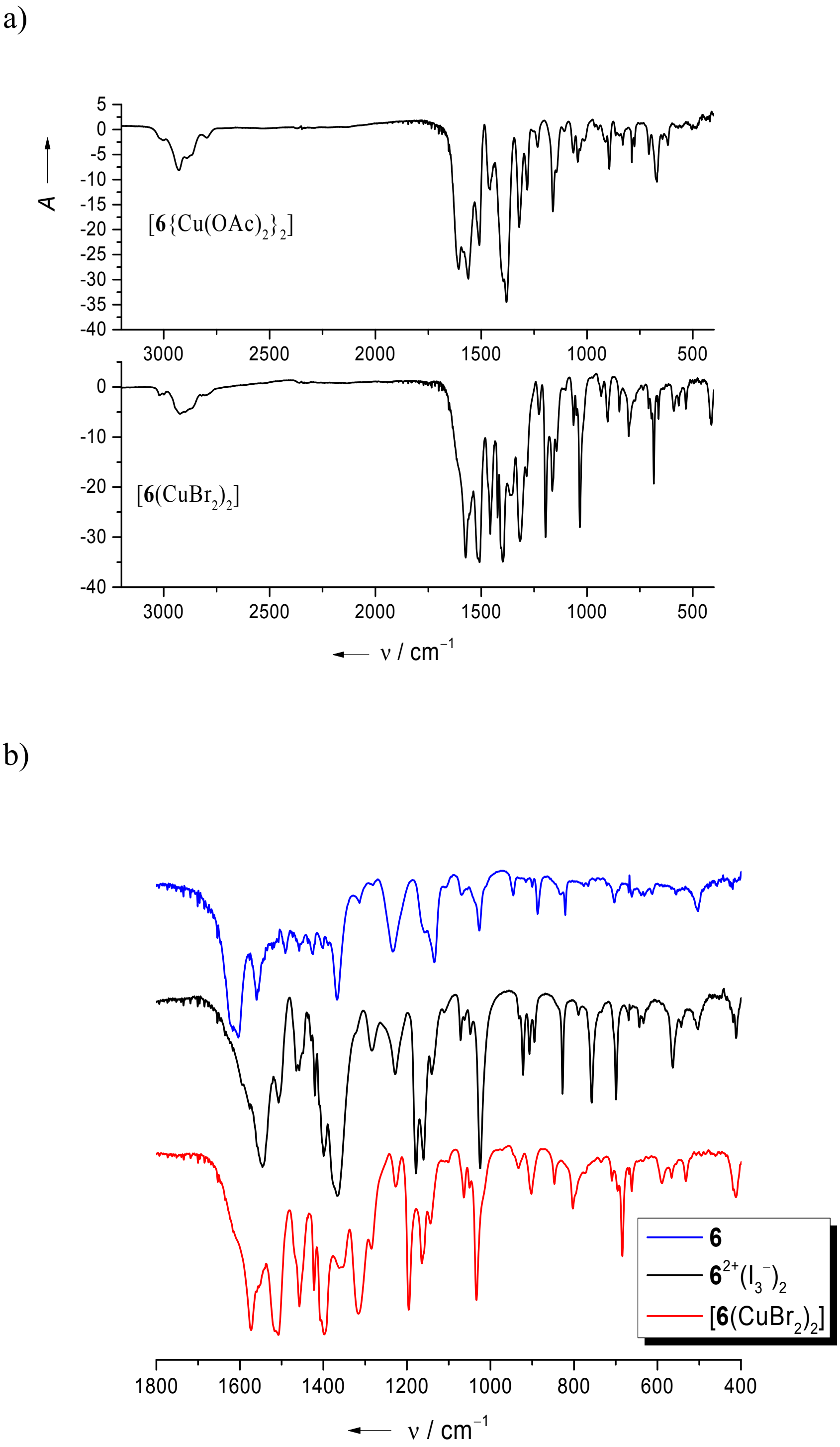

Figure S5. UV/Vis spectra of **6**$(I_3)_2$ and [**6**$(CuI)_2](I_3)_2$ dissolved in CH_3CN.

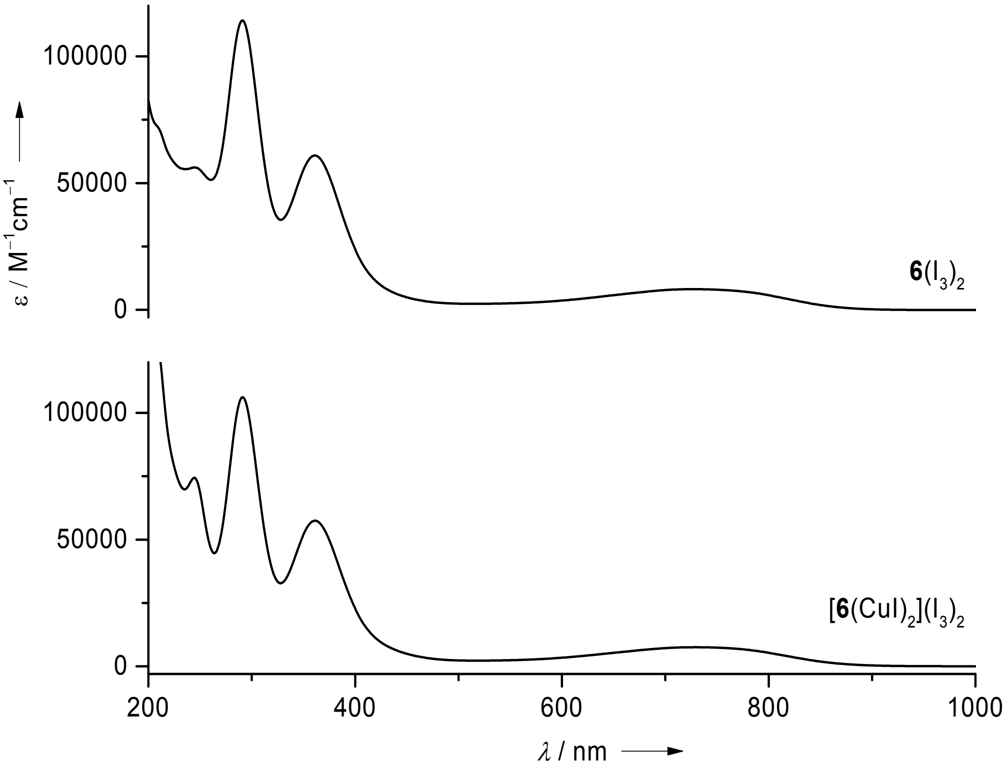

Figure S6. a) Structure of **6**$(PF_6)_2$ (prepared from **6** and $AgPF_6$). Hydrogen atoms omitted for clarity. Selected bond distances (in Å): N1-C1 1.323(3), N1-C6 1.353(3), N2-C6 1.341(3), N3-C6 1.340(3), N4-C3 1.351(3), N4-C11 1.327(3), N5-C11 1.362(3), N6-C11 1.352(3), C1-C2 1.441(3), C1-C5' 1.446(3), C2-C3 1.420(3), C3-C4 1.446(3), C4-C5 1.343(3). b) Structure of the salt **6**$(I_3)_2$. Hydrogen atoms omitted for clarity.

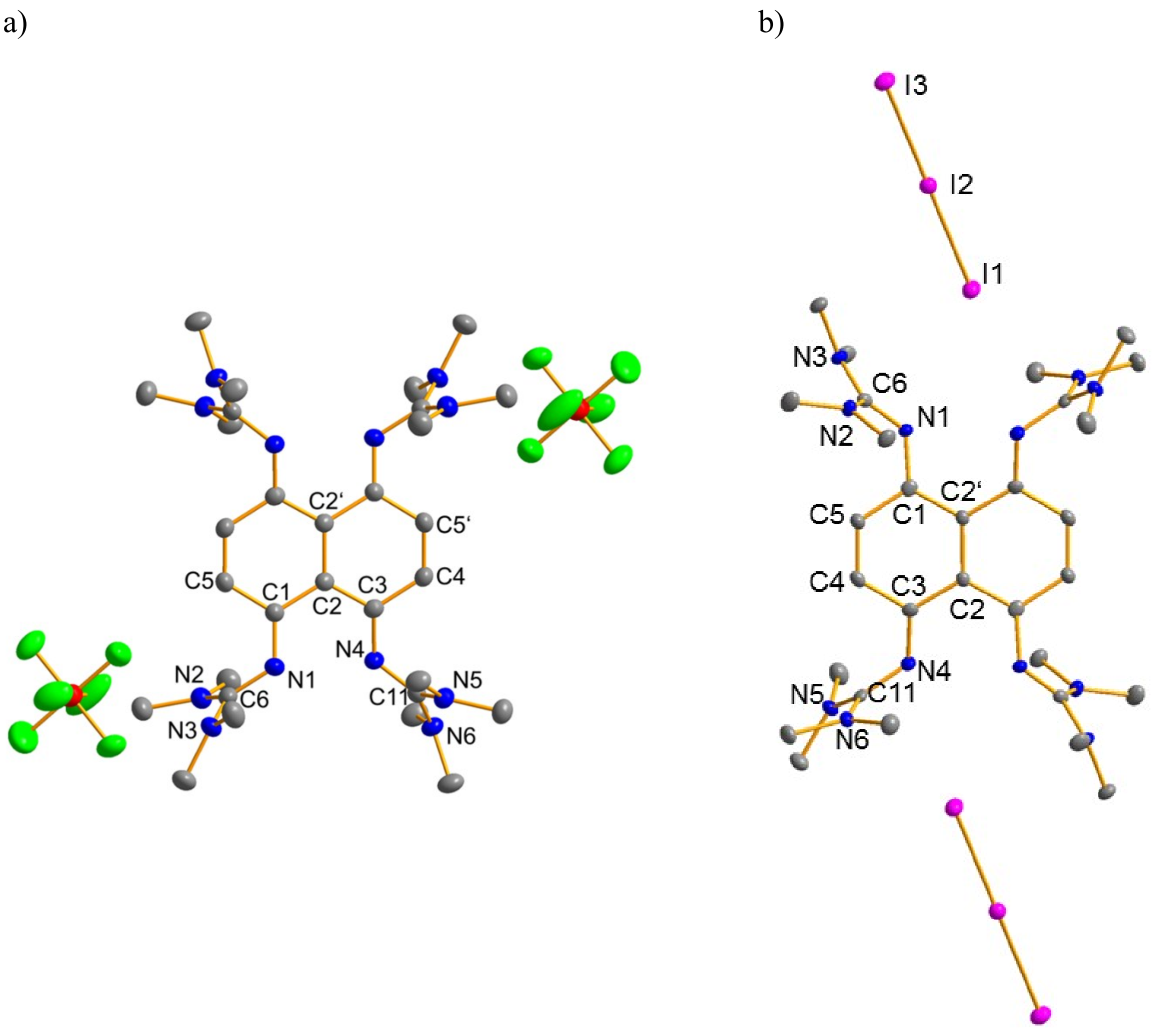

Crystal data for $[\mathbf{6}(PF_6)_2]\cdot CH_2Cl_2$, $C_{31}H_{52}Cl_2F_{12}N_{12}P_2$: $M\text{r} = 953.69$, 0.30 x 0.25 x 0.20 mm^3, monoclinic, space group P2(1)/n, $a = 12.794(3)$, $b = 8.0020(16)$, $c = 21.272(4)$ Å, $\beta = 96.49(3)°$, $V = 2163.8(8)$ Å^3, $Z = 2$, $d_{\text{calc}} = 1.464$ Mg·m^{-3}, Mo $K\alpha$ radiation (graphite monochromated, $\lambda = 0.71073$ Å), $T = 100$ K, θ_{range} 1.93 to 30.02°. Reflections measd. 11460, indep. 6281, $R_{\text{int}} = 0.0431$. Final R indices $[I > 2\sigma(I)]$: $R_1 = 0.0581$, w$R_2 = 0.1418$.

Figure S7. CV curves for [**6**(CuI)$_2$](I$_3$)$_2$ in CH$_3$CN (Ag/AgCl electrode, tetrabutylammonium-hexafluorophosphate as supporting electrolyte, potentials (E in V) given versus the redox couple Fc/Fc$^+$.

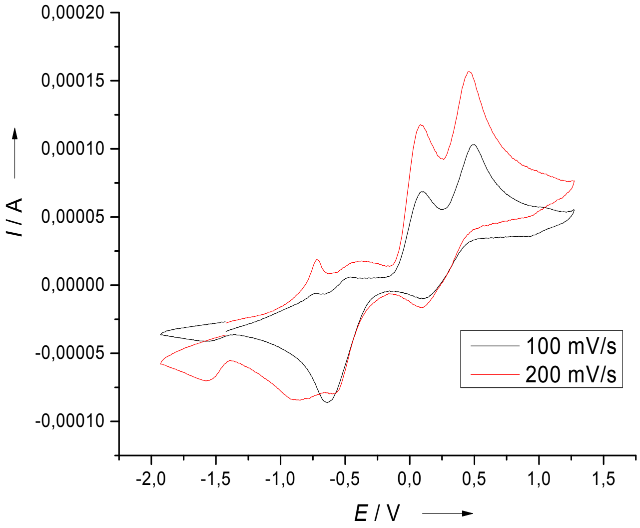

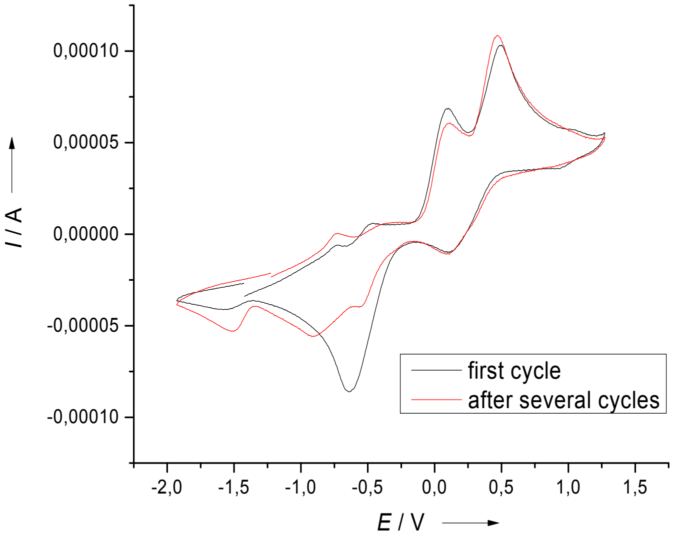

Figure S8. IR spectrum of **8** (KBr disk)

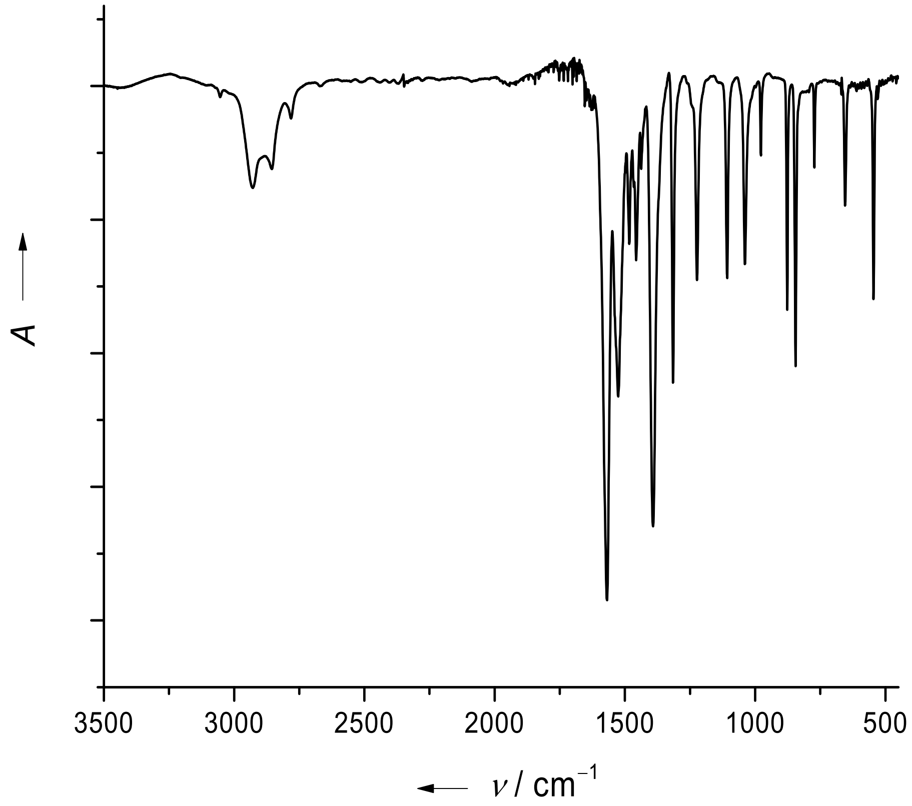

Summary of the results of the quantum chemical calculations

B3LYP/SV(P)

system	state	S*S	E/Hartee	E/eV
$[\mathbf{6}(CuI)_2]^{2+}$	Sz=0	0.318	-5704.444562842	0.0
	^3A	2.013	-5704.438532780	0.164
	^1A(RHF)	-	-5704.444328733	0.006
$[\mathbf{6}\{CuI(py)\}_2]^{2+}$	Sz=0	0.855	-6200.370141264	0.0
	^3A	2.009	-6200.367633708	0.068
	^1A(RHF)	-	-6200.365897629	0.115
$[\mathbf{6}\{CuI(CO)\}_2]^{2+}$	Sz=0	-	-	-
	^3A	2.010	-5930.793005285	0.405
	^1A(RHF)	-	-5930.807880047	0.0

BP/SV(P)

system	state	S*S	E/Hartee	E/eV
$[\mathbf{6}(CuI)_2]^{2+}$	Sz=0	0.231	-5706.725330637	0.0
	^3A	2.004	-5706.720483703	0.132
	^1A(RHF)	-	-5706.725169448	0.004
$[\mathbf{6}\{CuI(py)\}_2]^{2+}$	Sz=0	0.406	-6202.982206286	0.020
	^3A	2.003	-6202.979015694	0.107
	^1A(RHF)	-	-6202.982935788	0.0
$[\mathbf{6}\{CuI(CO)\}_2]^{2+}$	Sz=0	-	-	-
	^3A	2.003	-5933.206069671	0.247
	^1A(RHF)	-	-5933.215132055	0.0

Tested addition of *p*-dimethylamino-pyridine (DAP) to $[6(CuI)_2]^{2+}$

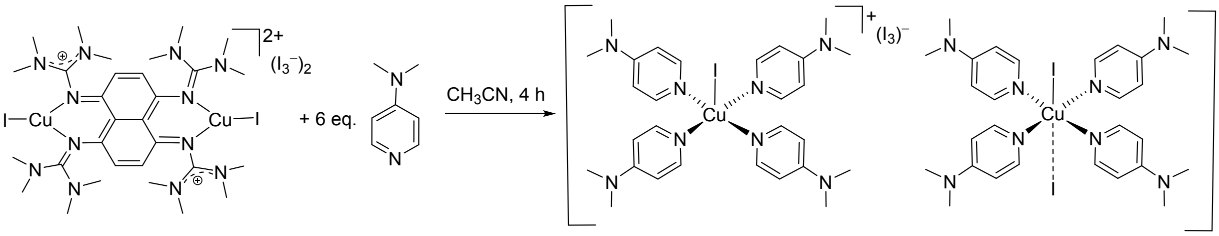

Scheme S1. Reaction between $[\mathbf{6}(CuI)_2]^{2+}(I_3^-)_2$ and *p*-dimethylamino-pyridine in CH_3CN yielded copper oxidation and GFA reduction. However, the Cu-GFA bond was cleaved. Please note that the reaction equation is not balanced, and other products are likely to be formed. The reactants are stated in the stoichiometry as used in the reaction.

Figure S9. Visualization of the structures of $[Cu(DAP)_4I][CuI_2(DAP)_4](I_3)$. Vibrational ellipsoids drawn at the 50% probability level. Hydrogen atoms omitted for sake of clarity. Colour code: Cyan Cu, Pink I, Grey C, Blue N.